Colloids and Surfaces B: Biointerfaces 141 (2016) 141–147

Contents lists available at ScienceDirect

Colloids and Surfaces B: Biointerfaces

journal homepage: www.elsevier.com/locate/colsurfb

Functionalized gold nanoparticles for topical delivery of methotrexate for the possible treatment of psoriasis

Hagar Bessar[a], Iole Venditti[b], Luisa Benassi[c], Cristina Vaschieri[c], Paola Azzoni[c], Giovanni Pellacani[c], Cristina Magnoni[c], Elisabetta Botti[d], Viviana Casagrande[e], Massimo Federici[e], Antonio Costanzo[d], Laura Fontana[b], Giovanna Testa[b], Fawzia Farag Mostafa[a], Samia Ali Ibrahim[a], Maria Vittoria Russo[b], Ilaria Fratoddi[b,*]

[a] Dermatology Department, Faculty of Medicine, Zagazig University, 44519, Sharkia, Egypt
[b] Department of Chemistry, University Sapienza of Rome, p.le Aldo Moro 5, 00185 Rome, Italy
[c] Department of Dermatology, University of Modena and Reggio Emilia, Italy
[d] Dermatology Unit, NESMOS Department, Sapienza University of Rome, Sant'Andrea Hospital, Via di Grottarossa 1037, 00189 Rome, Italy
[e] Department of Systems Medicine, University of Rome Tor Vergata, Rome, Italy

ARTICLE INFO

Article history:
Received 5 August 2015
Received in revised form
16 December 2015
Accepted 12 January 2016
Available online 16 January 2016

Keywords:
Hydrophilic gold nanoparticles
Drug loading
Methotrexate drug delivery
Functionalized nanoparticles

ABSTRACT

Gold nanoparticles (AuNPs) represent an effective choice for topical drug delivery systems thanks to their small size, general non-toxicity, ease of functionalization and high surface to volume ratio. Even if systemic, methotrexate still plays an important role in psoriasis treatment: its topical use shows insufficient percutaneus penetration owing to limited passive diffusion, high molecular weight and dissociation at physiological pH. The aim of our study was to design a new drug delivery nanocarrier for Methotrexate and to improve its solubility, stability and biodistribution. AuNPs were on purpose prepared with a hydrophilic stabilizing layer, in order to improve the colloidal stability in water. Water-soluble gold nanoparticles functionalized by sodium 3-mercapto-1-propansulfonate (Au-3MPS) were prepared and loaded with methotrexate (MTX). The loading efficiency of MTX on Au-3MPS was assessed in the range 70–80%, with a fast release (80% in one hour). The release was studied up to 24 h reaching the value of 95%. The Au-3MPS@MTX conjugate was fully characterized by spectroscopic techniques (UV–vis, FTIR) and DLS. Preliminary toxicity tests in the presence of keratinocytes monolayers allowed to assess that the used Au-3MPS are not toxic. The conjugate was then topically used on C57BL/6 mouse normal skin in order to trace the absorption behavior. STEM images clearly revealed the distribution of gold nanoparticles inside the cells. *In vitro* studies showed that Methotrexate conjugated with Au-3MPS is much more efficient than Methotrexate alone. Moreover, DL50, based on MTT analysis, is 20 folds reduced at 48 h, by the presence of nanoparticles conjugation. UV–vis spectra for *in vivo* tracing of the conjugate on bare mouse skin after 24 h of application, show increased delivery of Methotrexate in the epidermis and dermis using Au-3MPS@MTX conjugate, compared to MTX alone. Moreover we observed absence of the Au-3MPS in the dermis and in the epidermis, suggesting that these layers of the skin do not retain the nanoparticles. Based on our data, we found that the novel Au-3MPS@MTX conjugate is an effective non-toxic carrier for the satisfactory percutaneous absorption of Methotrexate and could help in possible topical treatment of psoriasis.

1. Introduction

Nanoparticle research is a fascinating branch of science that expressed an increasing interest due to a vast variety of promising applications in key impact technological areas. Among others, gold nanoparticles (AuNPs) exhibit a range of chemical-physical properties suitable for advanced applications such as sensing, [1–3] optoelectonics [4–6] biotechnology and nanomedicine from diagnosis to therapeutics, [7,8] and drug delivery systems, [9,10] also considering their possible toxicity. [11,12]

One of the main feature of AuNPs is that it is possible a fine control on their size, composition and functionality and among others stabilizing layers, thiol based ligands lead to a covalent, stable and chemically tunable layer. [13–15] In this context, the use of thiol stabilized AuNPs as drug delivery system is challenging.

One of the most common dermatological diseases is represented by psoriasis. Psoriasis is a common chronic persistent immune mediated inflammatory skin condition, affecting 2% of population, that leads to hyperproliferation of keratinocytes [16–18]. That

* Corresponding author. Fax: +39 6490324.
E-mail address: ilaria.fratoddi@uniroma1.it (I. Fratoddi).

http://dx.doi.org/10.1016/j.colsurfb.2016.01.021
0927-7765/

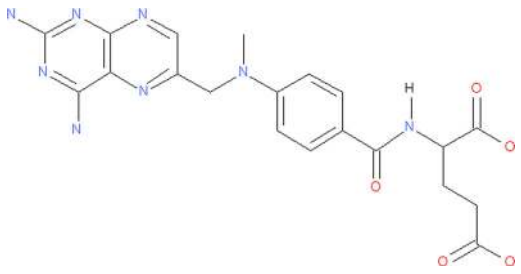

Fig. 1. Methotrexate (MTX) chemical structure.

hyper proliferative keratinocytes effect in thick epidermis clinically appears as thick, silvery scales and itchy, dry, salmon pink patches, mostly on elbows, knees and scalp but also in other cutaneous sites [19,20] giving rise to tiresome diseases; for example, a 5–8% of patients complains from psoriatic arthritis, which can be painful and greatly limits mobility [21].

Psoriasis is a multifactorial disease, with a polygenic background. It is believed that dendritic cells (DCs), keratinocytes and T cells play a major role in the pathogenesis of psoriasis. Indeed these cells are principally responsible for the production of a great variety of pro-inflammatory cytokines and chemokines, mainly interleukin (IL)-6, IL-23, IL-17, IL-21, tumor necrosis factor alpha. These inflammatory stimuli lead to keratinocytes hyperproliferation and autoamplification loop, with the formation of psoriasis plaques [22,23].

Treatment options depend on severity of psoriasis [24]. The main goal of treatment is to slowdown keratinocytes hyper proliferation and decrease inflammation by blocking specific inflammatory pathways. Many topical treatments are used with or without combination of other systemic treatments. Topical therapeutics include coal tar, corticosteroids, anthralin, retinoids, vitamin D3 analogues and tacrolimus plus several formulations which are expected to be used in enhancing approaches for drug delivery strategies [25].

Among others, methotrexate (MTX, reported in Fig. 1), is a folate antagonist, an allosteric inhibititor of dihydrofolate reductase (DHFR), well-known as an adjuvant for the treatment of various cancers and suited to inhibit dihydrofolate reductase in DHFR-based protein expression systems [26,27]. MTX is also effective in treatment of pyrimethamine-resistant Plasmodium vivax malaria parasites and shows immunosuppressive effects in, *e.g.*, rheumatoid arthritis [28]. However clinical studies have revealed that its effect was limited because it led to toxic dose-related side effects and because of the drug resistance of the tumor cells [29].

Stewart et al. and McCullough et al. suggested that localized Methotrexate has a limited passive diffusion, sufficient to affect psoriatic plaque when applied topically. This drug is characterized by high molecular weight and is mostly in dissociated form at physiological pH, with insufficient penetration into the basal layer of epidermis [30]. *In vivo* studies using topical MTX drug, revealed that the skin penetration of MTX is weak and the rate of absorption in rat skin of a MTX 1% acqueous solution is very low [31]. Biologic agents have been approved by the FDA to treat moderate to severe psoriasis that not responded to an adequate trial of one or more of the traditional drugs. Biologic therapies are most effective in the treatment of psorisis [32], but a percentage of no-responder patients still exists. Moreover, disadvantages are represented by their possible side effects and limited availability of long-term safety data. Based on PASI (Psoriasis Area and Severity Index) score, psoriasis can be classified in mild, moderate and severe [33–35]. The most frequent type is a mild psoriasis, which mainly requires topical treatment. In this context, methotrexate still has a golden role in psoriasis treatment [36–40].

An approach thus far is to design a drug delivery system for MTX in order to improve its solubility, *in vivo* stability and biodistribution [41,42].

Only few papers report on the therapeutic effects of AuNPs as carriers of MTX and in particular in psoriasis treatment; one approach is based on the immobilization of the drug on AuNPs surface by means of a direct synthesis approach: the MTX can be used as a ligand and reducing agent for a one pot procedure, demonstrating an enhanced therapeutic effect of conjugated MTX, with cytotoxic effects in choriocarcinoma cell lines [43]. Alternatively, processes based on post-synthesis immobilization can be used and the conjugate shows an higher efficiency compared with an equal dose of free MTX with cytotoxic effects; in particular it inhibits tumor growth in a mouse ascites model of Lewis lung carcinoma [44].

The present study aims at *in vitro* and *in vivo* investigation of the efficacy of the nanoparticles therapy in comparison to methotrexate as a standard chemotherapeutic agent for treatment of psoriasis using keratinocytes cell models and organotypic raft cultures. In this work the use of functionalized gold nanoparticels as MTX drug delivery system is proposed for topical psoriasis treatment. Considering the studies reported in the literature on the correlation between the size of AuNPs and penetration across human skin, and in particular on the barrier effect occurring for nanoparticles in the range 10–60 nm, [45] AuNPs with size below 10 nm have been selected.

In this context, MTX drug was immobilized onto functionalized gold nanoparticles; the loading and release kinetics were assessed and the new conjugate was tested on keratinocytes monolayer cell culture in order to evaluate the toxicity and proper dose. The conjugate, Au-3MPS and MTX alone were topically applied on C57BL/6 mouse normal skin in order to trace cutaneous absorption and drug delivery.

2. Materials and methods

2.1. Instruments

UV–vis spectra were run in H_2O solutions by using quartz cells, with a Varian Cary 100 Scan UV–vis spectrophotometer. Size distribution of AuNPs in H_2O solution have been investigated at the temperature of 25 °C by means of dynamic light scattering (DLS) technique by using a Malvern Nano ZS90 scattering apparatus (Malvern Zetasizer Nanoseries Instruments Ltd., Worcestershire, UK) on nanoparticle aqueous suspensions (0.01–0.20 mg/mL). [46]. Zeta potential has been measured by using Malvern NanoZS90 apparatus with disposable folded capillary cuvettes, provided with electrodes. [47,48] FTIR spectra have been recorded on cast deposited films from ethanol solutions using KRS-5 cells, with a Bruker Vertex 70 spectrophotometer. Field Emission Scanning Electron Microscopy (FE-SEM) images have been acquired with the Auriga Zeiss instrument (resolution 1 nm, applied voltage 6–12 kV) on freshly prepared films drop casted from H_2O solution on a metallic sample holder. Atomic Force Microscopy (AFM) images have been acquired with Veeco Instrument, model Icon with controller and Nanoscope 5Harmonix integrated system on freshly drop casted sample on Si/SiO_2 substrate. Scanvac-CoolSafe55-4 Lyophilizer has been used to dry samples. A Mini Spin–Eppendorf centrifuge was used for purification of AuNPs samples (13000 rpm, 20 min, 5× with deionized water). pH measurements were done with a CyberScan pH 600 (Eutech Instruments). Deionized water was obtained from Zeener Power I Scholar-UV (18.2 MΩ).

2.2. Materials

Deionized water has been degassed for 30 min with Argon, before use. Solvents: CH_2Cl_2, MeOH, EtOH, acetone, $CHCl_3$, HCl (Aldrich reagent grade) have been used as received. Sodium 3-mercapto-1-propanesulfonate ($HS(CH_2)_3SO_3Na$, 3MPS), 2-Diethylaminoethanethiol hydrochloride ($HSCH_2CH_2N(CH_2CH_3)_2{\cdot}HCl$, DEA), tetrachloroauric(III) acid

trihydrate ($HAuCl_4 \cdot 3H_2O$), sodium borohydride ($NaBH_4$) have been used as received (Aldrich reagent grade). Methotrexate (Sigma–Aldrich, M 8407, 4-Amino-10-methylfolic acid hydrate, MTX, $C_{20}H_{22}N_8O_5$ molecular weight is 545.44 g/mol) was purchased from Sigma–Aldrich. Methotrexate is practically insoluble in water. It dissolves in solutions of mineral acids (such as HCl) and in dilute solutions of alkali hydroxides. MTX solution was freshly prepared in water at pH 5.5 and stored in the dark at 4 °C until use. Locobase cream was purchased from Astellas Pharma Europe B.V. Gold nanoparticles functionalized with 3-mercaptopropane sulphonate (Au-3MPS) or 2-Diethylaminoethanethiol hydrochloride (Au-DEA), were prepared and characterized according to literature procedure [49,50]. Briefly, Au-3MPS and Au-DEA have been prepared with Au/thiol (Au/S) molar ratio 1/4 and 1/10 and the procedure is herein reported for Au/S 1/4 Au-3MPS sample. Starting from 200 mg of $HAuCl_4 \cdot 3H_2O$ in 20 mL of deionized water, a solution of 3MPS (340 mg in 20 mL of deionized water) was added. Under vigorous stirring the reducing agent $NaBH_4$ (190 mg in 20 mL of deionized water) has been added. The mixture was allowed to react at room temperature for 3 h and at the end, the brown solid was recovered and purified by centrifugation (13,000 rpm, 20 min, 5× with deionized water).

Au-3MPS (1/4) main characterizations: UV (λ_{max} [nm], H_2O): 530 nm; DLS ($2R_H$ [nm], H_2O): 4 ± 1 nm. FT-IR ν (cm^{-1}): ν_{as} (S═O)$_2$ = 1352, ν_a (S═O)$_2$ = 1190, ν (C—S) = 603. Yield (w/w) 31%.

Au-3MPS (1/10) main characterizations: UV (λ_{max} [nm], H_2O): 533 nm; DLS ($2R_H$ [nm], H_2O): 5 ± 1 nm. FT-IR ν (cm^{-1}): ν_{as} (S═O)$_2$ = 1352, ν_a (S═O)$_2$ = 1190, ν (C—S) = 603. Yield (w/w) 22%.

2.3. Loading of MTX on Au-3MPS

Bioconjugation was carried out following the non-covalent procedure already assessed in the literature [51], for similar compounds either on the 1/4 and 1/10 Au/S Au-3MPS samples [52,53]. In order to assess the loading, a calibration curve was done for MTX in H_2O (pH 5.5), with solutions in the concentration range 5.0×10^{-7}–5.0×10^{-5} M and the extinction coefficient at wavelength 302 nm was calculated equal to 19330 M^{-1} cm^{-1}. (UV–vis spectrum is reported in the Supporting Information, Fig. S1).

The loading was assessed on three separate tests and a mean value and SD were calculated. The procedure is briefly reported for the 1/4 sample: Au-3MPS nanoparticles (10 mg) were dissolved in water (4 mL pH 5.5) and vigorously stirred for 4 h at room temperature in the presence of MTX (2 mg) in order to have a weight ratio AuNPs/drug = 5/1. The reaction mixture was maintained in the dark to avoid MTX degradation with light. After 4 h, the mixture was purified by centrifugation (at room temperature, 13,000 rpm, 90 min) in order to separate the Au-3MPS@MTX conjugate from the free MTX in solution. Then 1 mL of the supernatant separated from the sediment was diluted in 100 mL of H_2O at pH 5.5 and analyzed for the drug content using UV–vis spectrophotometer at 302 nm [54]. By using the calibration curve it was possible to calculate the free MTX content and by difference the MTX loaded on the Au-3MPS $m(MTX_{loaded}) = m(MTX_{weighed}) - m(MTX_{free})$. The loading efficiency was calculated as $\eta = m(MTX_{loaded})/m(MTX_{weighed}) \times 100$, according to literature [55].

2.4. Release of MTX from Au-3MPS

The Au-3MPS@MTX conjugate was dried at 30 °C and the release was studied. 1 mg of the conjugate was dissolved in 100 mL of H_2O pH 5.5, and stirred at 37 °C. Withdrawal at different reaction times (30 min, 2, 4 and 24 h) were centrifuged (13,000 rpm, 15 min) and allowed to quantify MTX free drug in the surnatant by UV–vis spectroscopy. Experiments were carried out in triple and mean and SD values assessed. The release was also studied in the presence of Locobase cream, following this protocol: 2 mg of the conjugated mixed with 2 mg of Locobase cream under constant stirring (at room temperature, avoiding light irradiation) for 15 min until appearance of homogenous mixture; the mixture was dissolved in 20 mL of H_2O pH 5.5 and stirred at 37 °C. Withdrawal at different reaction times (30 min, 2, 4 and 24 h) were centrifuged (13,000 rpm, 15 min) and allowed to quantify MTX free drug in the surnatant by UV–vis spectroscopy.

2.5. In vitro *skin permeation tests*

2.5.1. Preparation of reagents

Methotrexate was dissolved in sodium carbonate buffer (pH 9.1) in order to obtain a 1 M solution suitable for cell tests (solution A). Then the solution A was diluted in buffered culture medium containing the phenol red indicator, till 100 mM concentration in order to form solution B. Then serial concentration from 100 μM to 6 mM were prepared from solution B.

Two different types of AuNPs were tested: Au-3MPS and Au-DEA. These were dissolved in 15 mL culture medium serum free. Prior to the *in vitro* test, the solution was passed through a 0.22 μm membrane filter. After filtration the concentration was 50 μg/mL. The Au-3MPS@MTX conjugate was dissolved as described before and filtration the concentration corresponded to 100 μM of MTX.

2.5.2. Primary keratinocytes culture

Normal human keratinocytes, obtained after excision of skin specimens from plastic surgery procedures, were prepared according to the method of Rheinwald and Green [56]. Skin was minced and trypsinized (0.25% trypsin, 0.02% EDTA) at 37 °C for 15 min after overnight incubation with dispase (Roche, Mannheim, Germany). Keratinocytes were grown in 75 cm^2 culture flasks (Costar, Cambridge, MA) with mitomycin-treated 3T3 mouse fibroblasts (10 mg/mL for 2 h at 37 °C; Sigma). The cells were cultured in Dulbecco's Modified Eagle's Medium/Ham's F12 Medium (DMEM/F12, 3:1) (Seromed-Biochrom KG, Berlin, Germany) containing insulin (5 μg/mL, Sigma), transferrin (5 μg/mL, Sigma), triiodothyronine (2 nM, Sigma), hydrocortisone (0.4 μg/mL, Sigma), adenine (180 mM, Sigma), mouse epidermal growth factors (EGF, 10 ng/mL, Sigma) 10% fetal calf serum (FCS, Serumed Biochrom) and 1.8 mM calcium. Subconfluent primary cultures were passed in secondary cultures for the following experiments.

2.5.3. MTT Test: 3-(4,5-Dimethylthiazol-2-yl)-2,5-diphenyltetrazolium bromide, a tetrazole test

The MTT assay is a colorimetric test for activity measurement of cellular enzymes widely used to measure cytotoxicity (loss of viable cells) or cytostatic activity (shift from proliferative to resting status) of potential medicinal agents.

2.5.3.1. Monolayer cultures. In this model keratinocytes from primary cultures are grown in serum-free and feeder-free conditions. Extracellular calcium supplementation at low concentration (0.1 mM) retain keratinocytes ability to form stratified epidermis. Cells from primary cultures were plated at 4.5 × 103/well in a 96 wells plate and grown in a serum free medium containing 0.4% bovine pituitary extract (BPE) (KGM, Lonza, Basel, Switzerland) until near confluence. At this time the cells were exposed with MTX at different concentrations (from 100 μM to 6 mM). Au-3MPS@MTX suspension was applied (from 0.05 μg/mL to 50 μg/mL) for 2 h, then rinsed with KGM and incubated at 37 °C for 46 additional hours.

After 48 and 72 h MTT test was performed: the cells were incubated with MTT solution (0.8 mg/mL) at 37 °C for 4 h. After this time they were dissolved in DMSO (200 μL/well) and the formazan dye formation was evaluated by scanning multiwell spectrophotometer at 550 nm. The results were expressed as viability percentage

respect of control. Results are calculated as the mean ± SD of three different experiments.

2.6. Sample preparation for Scanning Transmission Electron Microscopy

After being co-cultured with gold nanoparticles for 48 and 72 h, the cells were washed twice with PBS, harvested by trypsin treatment, fixed in 2.5% (v/v) glutaraldehyde solution and post fixed in aqueous osmium tetroxide. The samples were then dehydrated in a graded series of ethanol and embedded in DURCUPAN ACM epoxy resin. Ultrathin sections (60 nm) were contrasted with uranyl acetate and lead citrate and imaged by Nova NanoSEM 450, Scanning Transmission Electron Microscopy (STEM, Houston, TX 77084, USA) at an accelerating voltage of 30 kV.

2.7. Preparation of cream formulation

The Locobase cream was mixed with freshly prepared Au-3MPS@MTX conjugate following this procedure: 100 μg of the conjugate (containing 16 μg of MTX) were mixed with 1 mg of Locobase cream under constant manual stirring at room temperature avoiding light irradiation for 15 min until appearance of homogenous mixture. The MTX was mixed with the Locobase by following the same procedure, by mixing 16 μg of MTX with 1 mg of Locobase cream. The formulations were then preserved at −20 °C

2.8. In vivo mice skin permeation

Eight-week-old wild-type mice (Harlan, Udine, Italy), all on C57BL/6 background, were used for the *in vivo* experiments. Mice were maintained in standard animal cages under specific pathogen-free conditions in the animal facility. Experiments were approved by the local ethics committee.

Mice were shaved on both flanks and used for application of the cream containing Au-3MPS@MTX conjugate on one flank while the other flank was treated by the same amount of cream containing Au-3MPS alone or Au-3MPS@MTX conjugate and cream containing MTX alone. The treated parts were covered with and adhesive tape to allow contact time. After 24 h mice were sacrificed and two skin biopsies were taken from both treated areas. One biopsy was used to trace MTX in the whole skin. The other biopsy was enzymatically separated by overnight incubation with dispase II (Roche Diagnostics, Milan, Italy) to obtain epidermis and dermis in order to trace the drug in both compartments, separately. The supernatant from the skin treated with Au-3MPS@MTX and reacted for 24 h with the dispase II enzyme was tested by UV–vis spectrophotometer for tracing the presence of MTX and AuNPs. Moreover, epidermis and dermis samples were incubated in acidic solution (1 mL of HCl 2 M) for 30 min, centrifuged (10 min, 13,000 rpm) and tested by UV–vis spectrophotometer for tracing the presence of MTX. Each part was taken separately for UV–vis measurements.

3. Results and discussion

Few literature reports deal with gold nanoparticles effects on cultures of skin-derived cell lines [57] and gold nanoparticle penetration (less than 15 nm) in thawed human skin [58,59]. In our research, colloidal stable gold nanoparticles have been prepared with 3MPS thiol as functionalizing layer, following the hereafter reported synthetic scheme (see Fig. 2a); the purification steps allowed to obtain gold nanoparticles with a narrow mean hydrodynamic diameter equal to 4 ± 1 nm, as confirmed by DLS technique (Fig. S2).

The UV–vis spectrum (Fig. 2b) of the Au-3MPS nanoparticles showed a Plasmon resonance at about 530 nm, typical of low diameter gold nanoparticles [60,61].

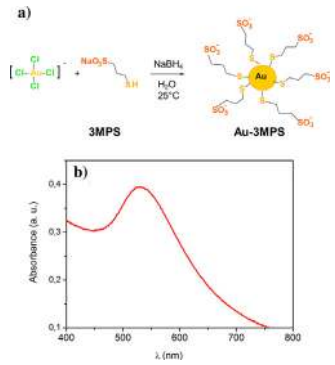

Fig. 2. a) reaction scheme; b) UV–vis spectrum in water of Au-3MPS nanoparticles.

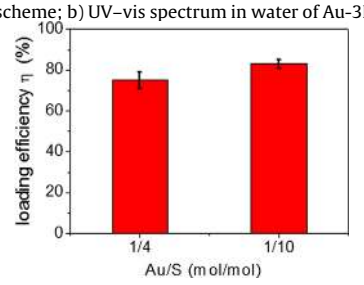

Fig. 3. Loading efficiency for Au-3MPS samples prepared with Au/S = 1/4 and 1/10. The error bar represent the SD value calculated on three different samples.

Au-3MPS@MTX conjugate was prepared and characterized in order to assess the interaction between AuNPs and MTX drug. The synthetic protocol is based on a non-covalent interaction and UV–vis spectroscopy was used to obtain quantitative loading data. In general, non-covalent methods (electrostatic adsorption or hydrophobic interactions) are reported as simple and effective approaches for drugs bioconjugation, in the presence of functionalized AuNPs. Thanks to the relatively weak affinity of the gold surface and/or the presence of thiol stabilizing layer, several drugs can be adsorbed, with a general retention of the therapeutic activities [62–64].

A weight ratio between Au-3MPS and MTX drug equal to 5/1 was chosen on the basis of literature report on different loaded drugs [65] and on our previous studies on similar nanoparticles [51] and the obtained mixture was deeply purified in order to remove the free drug. The loading was carried out either on 1/4 and 1/10 Au/S samples in order to compare and optimize the loading process. The loading efficiency was calculated on three different samples for Au-3MPS 1/4 sample equal to $\eta = 75 \pm 4\%$, value higher if compared with other carriers reported in the literature [66,67]. In the case of Au-3MPS 1/10 sample an higher loading efficiency was obtained ($\eta = 83 \pm 2\%$) and in Fig. 3 the loading efficiency of the samples is compared. It can be observed that within the standard deviation values, an higher loading efficiency occurs for the more functionalized Au/S 1/10 sample, even though the purification steps became more tedious when high quantities of thiol are used. The stability of the conjugate was assessed for a period as long as 6 months by means of DLS and Z-potential techniques on lyophilized samples maintained at 4 °C (Au-3MPS@MTX fresh sample Z-potential −32 ± 1 mV; Au-3MPS@MTX after 6 month Z-potential −30 ± 2 mV).

Au-3MPS@MTX was studied through FT-IR spectroscopy and an interaction was evidenced from the peaks analysis. The FT-IR spectra (reported in Fig. S3 for MTX drug and Au-3MPS@MTX conjugate, respectively) confirmed the presence of MTX in the conjugate with the typical absorption peaks at 3059 and 2951 cm^{-1} due to the carboxylic group and the C—N and NH_2 vibrational modes at 1685, 1616, 1389 and 1073 cm^{-1}. In particular the amide groups was observed at 1684 cm^{-1} for the free MTX [68] and at 1614 cm^{-1} in the conjugate. Zeta potential studies on the conjugate were carried

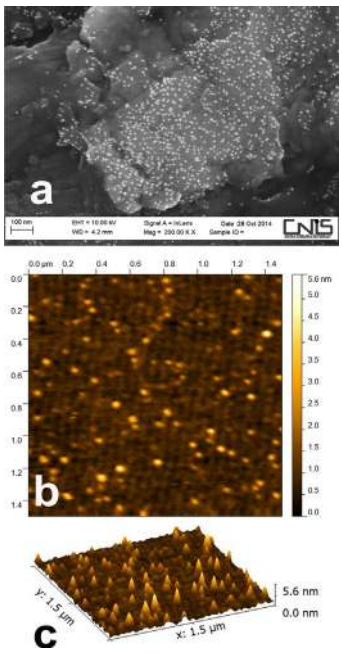

Fig. 4. a) FESEM image of Au-3MPS@MTX bioconjugate; b) and c) AFM images of Au-3MPS@MTX bioconjugate.

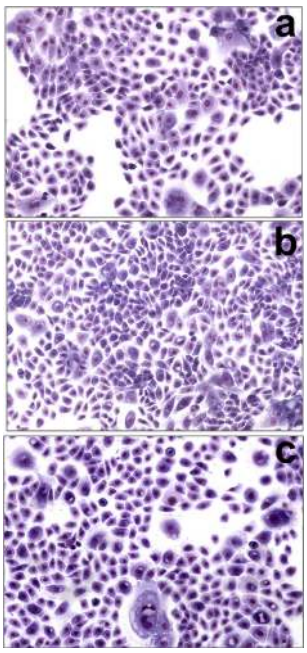

Fig. 5. Normal human Keratinocytes cultured for 48 h: (a) Control untreated; (b) cultured with 40 μg/mL Au-3MPS; (c) cultured with 40 μg/mL Au-DEA (10× magnification).

out to achieve information on the stability By comparing the data of Au-3MPS and Au-3MPS@MTX, the Z-potential value evidenced a small decrease (from -27 ± 3 mV in the Au-3MPS to -32 ± 1 mV in the conjugate), as a result of water stable samples up to 6 months (see Fig. S5).

The morphology of the conjugate was observed by FE-SEM and AFM microscopies and no modifications in the Au-3MPS morphology upon interaction with MTX was observed. It is noteworthy that no aggregated structures were observed. In Fig. 4a–c the FE-SEM and AFM images of the Au-3MPS@MTX conjugate are reported. It can be noticed that quite regular size nanoparticles with diameters of about 5 nm are obtained at the solid state, confirming the hydrodynamic DLS data.

An important point to be assessed in view of dermatological applications is the release kinetic of the MTX drug. From our studies we found that about 80% of the MTX was released from the Au/S 1/4 Au-3MPS sample after one hour and that in 24 h the release was up to 95% in PBS buffer (see Fig. S6). The release kinetics has been also studied in the presence of Locobase cream evidencing a slower release with respect to PBS buffer medium: about 70% in 24 h. By comparison, the release kinetic was also studied for the Au/S 1/10 sample and a quite similar release was observed. Au-3MPS prepared with the Au/S molar ratio 1/4 sample have then been used for the *in vitro* skin permeation and *in vivo* mice skin permeation tests considering the better yield in the preparation and purification steps.

3.1. In vitro *skin permeation tests*

In order to exclude the toxic conditions of nanoparticles during keratinocytes treatment and to ensure the optimum low doses, we first investigated different concentrations by application of a series of control experiments.

3.2. *Morphology of keratinocytes after Au-3MPS and Au-DEA treatment*

Two types of AuNPs were tested in the presence of keratinocytes for possible toxicity and to select the non or less nanocarrier toxicity [69]. As shown in Fig. 5 the cells do not display changes after treatment with Au-3MPS nanoparticles when compared (Fig. 5b) to the control group (Fig. 5a). Keratinocytes were normal in shape, suggesting that the Au-3MPS alone are not toxic for the cells. Similarly, results of the MTT test, regarding the incubation of cells with different concentration of Au-3MPS ranging from 0.05 μg/mL to 50 μg/mL, for 48 h, had no significant changes on cell viability in comparison to the untreated negative control (Fig. 6a).

The morphology of keratinocytes was observed also in the presence of different concentration of Au-DEA nanoparticles; in that case, some toxic effects were observed and this prompted us to select the Au-3MPS system for further investigations. The effect on normal human keratinocytes cultured for 48 h with 40 μg/mL Au-DEA is shown in Fig. 5c.

3.3. *Growth inhibitory effect of methotrexate and tests on Au-3MPS@MTX*

Preliminary studies were carried out to choose the proper solvent for the drug. Therefore, the MTX was dissolved in sodium carbonate buffer (pH 9.1) in order to obtain a solution suitable for cell tests. The effect of MTX on normal human keratinocytes was studied after 48 and 72 h at different concentrations. As shown in Fig. 6b the inhibitory effect of MTX showed a significant decrease in the percentage of viability at 48 h with a DL50 (Median Lethal Dose) 750 μM. After 72 h (Fig. 6b) treatment the DL50 was 200 μM. These results show that the MTX growth inhibition has been observed after 48 and 72 h. At 24 h no toxic effect was observed (data not shown).

Our studies were performed to carefully select the most appropriate conditions for preparing MTX loaded Au-3MPS. Moreover, investigations were carried out to choose the sonication time that was fixed at 1 min. As the nanoparticles have a capacity to release the MTX in about two hours, we have set up our experiments taking into account this fact. Therefore, two sets of experiments were made. For the preliminary keratinocytes experiment, we treated the cells with different concentrations of Au-3MPS@MTX for two hours. At the end of this time the medium was removed and replaced with fresh medium. The cells were then left in culture until they reached 48 and 72 h. The results, shown in Fig. 6c highlighted that MTX conjugated with Au-3MPS is much more efficient than

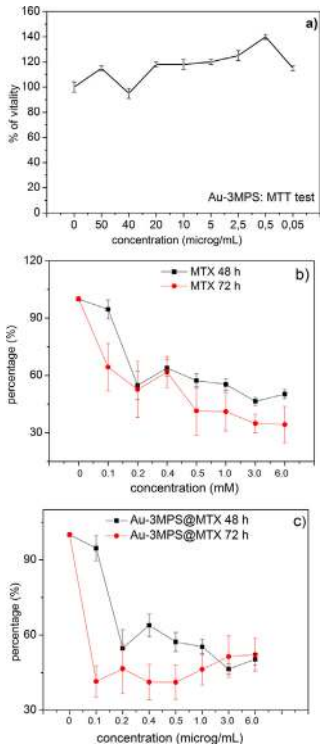

Fig. 6. MTT tests: (a) Viability of keratinocytes incubated with different concentrations of Au-3MPS after 48 h compared with untreated keratinocytes. The results are expressed as viability percentage respect of control; (b) inhibition of cell vitality of MTX at different concentrations after 48 h show a DL50 corresponding to 1 mM. After 72 h DL50 was 450 μM; (c) Au-3MPS@MTX was applied for 2 h, then removed and the cells incubated with fresh medium for an additional time of 46 h and 70 h. DL50 resulted 50 μg/mL and 10 μg/mL at 48 and 72 respectively. Error bars quote the standard deviation of at least three independent measurements.

MTX alone. Moreover DL50 is twenty folds reduced at 72 h by the presence of nanoparticles conjugation. This result is in agreement with data reported by Chen et al. for tumor cell lines [43] and for the first time we demonstrated the same behavior also on normal human keratinocytes.

3.4. 10Cell morphology observed by STEM

STEM study has been carried out on Au-3MPS@MTX and control in order to assess the cell internalization of gold nanoparticles in human keratinocytes. As reported in Fig. 7a and b, where the control cultured cell is compared with cell treated with the bioconjugate, the Au-3MPS@MTX are internalized as indicated by the black arrows. The cell shows mitochondrial vacuolization and filaments fragmentation demonstrating that is enough only one application of 2 h of NP to allow them to penetrate inside the cells.

3.5. In vivo *mouse skin permeation*

The *in vivo* capability of Au-3MPS@MTX conjugate to penetrate and release MTX in the skin, was evaluated separately in epidermal and dermal skin compartments. Control tests in *in vivo* studies of MTX drug, reported in the literature revealed that the skin penetration of MTX is weak and the rate of absorption in rat skin of a 1% acqueous solution of MTX is low. [31] In order to study MTX skin penetration, *in vivo* mice skin was topically treated with Au-3MPS@MTX conjugate or to MTX aloneAfter 24 h skin biopsy from both treated areas was used for UV–vis analysis to trace the MTX content. We made an investigation of the absorbance peaks of the supranatants recovered from the skin treated with Au-3MPS@MTX or MTX alone and reacted for 24 h with the dispase enzyme, which allowed to separate epidermis from dermis. UV–vis spectra analysis of the samples treated with the formulation based

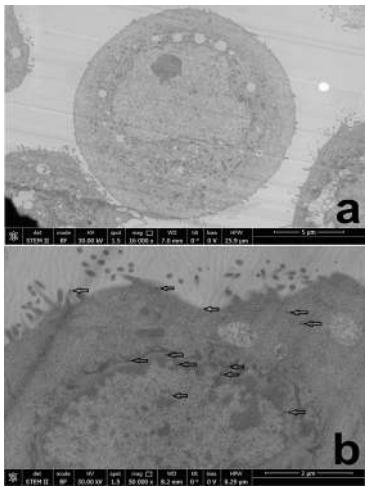

Fig. 7. STEM images of normal human keratinocytes. a) control cells cultured for 72 h; b) treated cells with 50 mg/mL Au-3MPS@MTX. The photograph illustrates the internalization of gold nanoparticles inside the cells (membrane, cytoplasm and nuclear envelope and in the nucleus) as indicated by the arrows.

on Au-3MPS@MTX, show that MTX drug can be observed both in the epidermis and, at less intensity, also in the dermis. On the contrary, samples treated with the formulation based on MTX alone, show a MTX peak in the epidermis while in dermis it was absent, suggesting deeper penetration of the drug into the skin using the gold nanoparticles as drug carrier (see Fig. S4a, c in the Supporting Information). Considering the dispase enzymatic reaction done for the skin separation, a quantitative determination was not possible considering also the decomposition of the drug occurring during the enzymatic treatment.

We also performed an experiment, by using the formulation based on Au-3MPS@MTX or Au-3MPS alone; nanoparticles were not observed by UV–vis spectra neither in the dermis nor in the epidermis, suggesting that both layers of the skin do not retain the nanoparticles. (see Fig. S4a, b in the Supporting Information).

In conclusion, these results confirm a deeper penetration of drug into the skin using the gold nanoparticles as drug carrier than the MTX alone, opening fascinating perspective for the application of Au-3MPS@MTX in cream formulation for dermatology diseases.

4. Conclusions

Nanoparticles skin penetration is a multifactorial and multistep process that involves a number of factors including the skin model, skin barrier integrity and the inherent physiochemical attributes of NP (size, shape, surface charge, etc.) and the vehicle of the formulation. However the evidence whether nanoparticle can penetrate into underlying tissue is still conflicting. Water-soluble gold nanoparticles functionalized by sodium 3-mercapto-1-propansulfonate (Au-3MPS) were prepared and loaded with methotrexate (MTX). The loading efficiency of MTX on Au-3MPS was assessed in the range 70–80%, with a fast release (80% in one hour). The release was studied up 24 h giving a value of 95%. The Au-3MPS@MTX conjugate was fully characterized by spectroscopic techniques (UV–vis, FTIR) and DLS and preliminary toxicity tests in the presence of keratinocytes allowed to assess the absence of toxicity of the used Au-3MPS. The effect of Au-3MPS@MTX on normal human keratinocytes *in vitro* has been investigated. Cells were incubated with different doses of MTX-AuNP and free MTX. Keratinocytes co-cultured with Au-3MPS@MTX did not exhibited marked changes showing that this concentration was not toxic for keratinocytes. DL50 was 20-folds reduced at 48 h by the presence of AuNPs. Electron microscopy studies have demonstrated that Au-3MPS@MTX are able to penetrate keratinocytes in culture. Moreover in a mouse model, an absorption due to the MTX drug

can be observed either in the epidermis and, in less intensity, also in the dermis. Overall results obtained in this work have shown that Au-3MPS are a promising carrier for MTX. This study has demonstrated a preliminary proof of percutaneous adsorption of low size gold nanoparticles. Although further *in vivo* studies are necessary to confirm the permeation of the skin barrier, the observation of MTX penetration in dermis, where psoriasis inflammatory infiltrate resides, suggests that Au-3MPS@MTX formulation could be suitable as topical therapy in psoriasis patients.

Acknowledgments

The authors gratefully acknowledge the Sapienza University of Rome, Ateneo Sapienza 2014/C26A14FCZP, 2015/C26A15H5J9 and 2015/C26A15LRMA projects for financial support. Antonio Costanzo work is supported by grants from AIRC, Telethon, National Psoriasis Foundation and ASPIRE. Ilaria Fratoddi acknowledges the Dept. of Chemistry, Sapienza University of Rome, for Support Research Initiative.

Appendix A. Supplementary data

Supplementary data associated with this article can be found, in the online version, at http://dx.doi.org/10.1016/j.colsurfb.2016.01.021.

References

[1] K. Saha, S.S. Agasti, C. Kim, X. Li, V.M. Rotello, Chem. Rev. 112 (2012) 2739–2779.
[2] I. Venditti, I. Fratoddi, M.V. Russo, A. Bearzotti, Nanotechnology 24 (2013) 155503.
[3] I. Fratoddi, A. Macagnano, C. Battocchio, E. Zampetti, I. Venditti, M.V. Russo, A. Bearzotti, Nanoscale 6 (2014) 9177–9184.
[4] J. Lawrence, J.T. Pham, D.Y. Lee, Y. Liu, A.J. Crosby, T. Emrick, ACS Nano 8 (2014) 1173–1179.
[5] E. Pedrueza, J. Sancho-Parramon, S. Bosch, J.L. Valdés, J.P. Martinez-Pastor, Nanotechnology 24 (2013) 065202.
[6] R.P. Kurta, L. Grodd, E. Mikayelyan, O.Y. Gorobtsov, I.A. Zaluzhnyy, I. Fratoddi, I. Venditti, M.V. Russo, V. Sprung, I.A. Vartanyants, S. Grigorian, Phys. Chem. Chem. Phys. 17 (2015) 7404–7410.
[7] D. Van Haute, J.M. Longmate, J.M. Berlin, Adv. Mater. 27 (2015) 5158–5164.
[8] S. Guo, L. Huang, Biotechnol. Adv. 32 (2014) 778–788.
[9] I. Fratoddi, I. Venditti, C. Cametti, M.V. Russo, J. Mater. Chem. B 2 (2014) 4204–4220.
[10] E.E. Connor, J. Mwamuka, A. Gole, C.J. Murphy, M.D. Wyatt, Small 1 (2005) 325–327.
[11] I. Fratoddi, I. Venditti, C. Cametti, M.V. Russo, Toxicol. Res. 4 (2015) 796–800.
[12] I. Fratoddi, I. Venditti, C. Cametti, M.V. Russo, Nano Res. 8 (2015) 1771–1799.
[13] D.E. Jiang, Nanoscale 5 (2013) 7149–7160.
[14] F. Vitale, R. Vitaliano, C. Battocchio, I. Fratoddi, E. Piscopiello, L. Tapfer, M.V. Russo, J. Organomet. Chem. 693 (2008) 1043–1048.
[15] P. Zhao, N. Li, D. Astruc, Coord. Chem. Rev. 257 (2013) 638–665.
[16] M.A. Lowes, M. Suarez-Farinas, J.G. Krueger, Annu. Rev. Immunol. 32 (2014) 227–255.
[17] M.S. Roberts, K.A. Walters, Human skin morphology and dermal absorption, in: M.S. Roberts, K.A. Walters (Eds.), Dermal Absorption and Toxicity Assessment, Informa Healthcare, New York, 2008, pp. 1–15.
[18] A. Nasir, Clin. Dermatol. 28 (2010) 458–466.
[19] C. Pfohler, C.S. Muller, T. Vogt, Curr. Rheumatol. Rev. 9 (2013) 2–7.
[20] F.O. Nestle, D.H. Kaplan, J. Barker, Psoriasis, N. Engl. J. Med. 361 (2009) 496–509.
[21] E. Chrustopothers, U. Mrowietz, Psoriasis, in: I.M. Freedberg, A.Z. Eisen, K. Wolff (Eds.), Fitzpatrick's Dermalology in General Medicine, vol. 1, 5th edition, McGraw-Hill, New York, 1999.
[22] E. Botti, G. Spallone, R. Caruso, G. Monteleone, S. Chimenti, A. Costanzo, Curr. Pharm. Biotechnol. 13 (2012) 1861–1867.
[23] F. Lacarrubba, G. Pellacani, S. Gurgone, A.E. Verzi, G. Micali, Int. J. Dermatol. 54 (6) (2015) 626–634.
[24] L. Naldi, D. Gambini, Clin. Dermatol. 25 (2007) 510–518.
[25] Y.H. Su, J.Y. Fang, Expert Opin. Drug Deliv. 5 (2008) 235–249.
[26] J. Jolivet, K.H. Cowan, G.A. Curt, N.J. Clendeninn, B.A. Chabner, N. Engl. J. Med. 309 (1983) 1094–1104.
[27] C. Neves, R. Jorge, A. Barcelos, Acta Reumatol. Port. 34 (2009) 11–34.
[28] C. Roubille, V. Richer, T. Starnino, C. McCourt, A. McFarlane, P. Fleming, S. Siu, J. Kraft, C. Lynde, J. Pope, W. Gulliver, S. Keeling, J. Dutz, L. Bessette, R. Bissonnette, B. Haraoui, Ann. Rheum. Dis. 74 (2015) 480–489.
[29] C.Y. Zhang, C.Y. Feng, Y. Yu, W.J. Sun, J. Bai, F. Chen, S.B. Fu, Basic Clin. Pharmacol. Toxicol. 99 (2006) 141–145.
[30] J.L. McCullough, D.S. Synder, G.D. Weinstein, A. Friedland, B. Stein, J. Invest. Dermatol. 66 (1976) 103–107.
[31] V. Dubey, D. Mishra, T. Dutta, M. Nahar, D.K. Saraf, N.K. Jain, J. Controlled Release 123 (2007) 148–154.
[32] A.W. Armstrong, J. Bagel, A.S. Van Voorhees, A.D. Robertson, P.S. Yamauchi, JAMA Dermatol. 151 (2015) 432–438.
[33] A. Menter, A. Gottlieb, S.R. Feldman, A.S. Van Voorhees, C.L. Leonardi, K.B. Gordon, M. Lebwohl, J.Y. Koo, C.A. Elmets, N.J. Korman, K.R. Beutner, R.J. Bhushan, Am. Acad. Dermatol. 58 (2008) 826–850.
[34] D.M. Pariser, J. Bagel, J.M. Gelfand, N.J. Korman, C.T. Ritchlin, B.E. Strober, A.S. Van Voorhees, M. Young, S. Rittenberg, M.G. Lebwohl, E.J. Horn, Arch. Dermatol. 17 (2007) 239–242.
[35] S.P. Raychaudhuri, J. Gross, Pediatr. Dermatol. 17 (2000) 174–178.
[36] R.E. Kalb, B. Strober, G. Weinstein, M. Lebwohl, J. Am. Acad. Dermatol. 60 (2009) 824–837.
[37] L. Sanchez-del-Campo, M.F. Montenegro, J. Cabezas-Herrera, J.N. Rodriguez-Lopez, Pigment Cell Res. 22 (2009) 588–600.
[38] P.K. Lakshmi, G.S. Devi, S. Bhaskaran, S. Sacchidanand, Indian J. Dermatol. Venereol. Leprol. 73 (2007) 157–161.
[39] I. Goma, S.E. Ali, T.A. El-Tayeb, Abdel-kader, MH, Photodiagn. Photodyn. Ther. 9 (2012) 362–368.
[40] A.A. Abdelbary, M.H.H. AbouGhaly, Int. J. Pharm. 485 (2015) 235–243.
[41] J.J. Liang, Y.Y. Zhou, J. Wu, Y. Ding, Curr. Drug Metab. 15 (2014) 620–631.
[42] C.S.J. Campbell, L.R. Contreras-Rojas, M.B. Delgado-Charro, R.H. Guy, J. Controlled Release 162 (2012) 201–207.
[43] N.T.T. Tran, T.H. Wang, C.Y. Lin, Y. Tai, Biochem. Eng. J. 78 (2013) 175–180.
[44] Y.H. Chen, C.Y. Tsai, P.Y. Huang, M.Y. Chang, P.C. Cheng, C.H. Chou, D.H. Chen, C.R. Wang, A.L. Shiau, C.L. Wu, Mol. Pharm. 4 (2007) 713–722.
[45] D.C. Liu, A.P. Raphael, D. Sundh, J.E. Grice, H.P. Soyer, M.S. Roberts, T.W. Prow, J. Nanomater. (2012), Article ID 721706.
[46] C. Cametti, I. Fratoddi, I. Venditi, M.V. Russo, Langmuir 27 (2011) 7084–7090.
[47] I. Venditti, I. Fratoddi, C. Palazzesi, P. Prosposito, M. Casalboni, C. Cametti, C. Battocchio, G. Polzonetti, M.V. Russo, J. Colloid Interface Sci. 348 (2010) 424–430.
[48] I. Fratoddi, I. Venditti, C. Battocchio, G. Polzonetti, C. Cametti, Nanoscale Res. Lett. 6 (98) (2011) 8.
[49] F. Vitale, R. Vitaliano, C. Battocchio, I. Fratoddi, C. Giannini, E. Piscopiello, A. Guagliardi, A. Cervellino, G. Polzonetti, M.V. Russo, L. Tapfer, Nanoscale Res. Lett. 3 (2008) 461–467.
[50] I. Venditti, C. Palocci, L. Chronopoulou, I. Fratoddi, L. Fontana, M. Diociaiuti, M.V. Russo, Colloids Surf. B 131 (2015) 93–101.
[51] N.K. Singh, S.K. Singh, D. Dash, B.P.D. Purkayastha, J.K. Roy, P. Maiti, J. Mater. Chem. 22 (2012) 17853–17863.
[52] I. Venditti, L. Fontana, I. Fratoddi, C. Battocchio, C. Cametti, S. Sennato, F. Mura, F. Sciubba, M. Delfini, M.V. Russo, J. Colloid Interface Sci. 418 (2014) 52–60.
[53] I. Fratoddi, I. Venditti, C. Cametti, C. Palocci, L. Chronopoulou, M. Marino, F. Acconcia, M.V. Russo, Colloids Surf. B 93 (2012) 59–66.
[54] J.A. Ciekot, T. Goszczy, J.B. Tomasz, Drug Res. 69 (2012) 1342–1346.
[55] J.A. Ankrum, O.R. Miranda, K.S. Ng, D. Sarkar, C. Xu, J.M. Karp, Nat. Protoc. 9 (2014) 233–245.
[56] J.C. Rheinwald, H. Green, Cell 6 (1975) 331–343.
[57] P. Ghosh, G. Han, M. De, C.K. Kim, V.M. Rotello, Adv. Drug Deliv. Rev. 60 (2008) 1307–1315.
[58] F.L. Filon, M. Crosera, G. Adami, M. Bovenzi, F. Rossi, G. Maina, Nanotoxicology 5 (2011) 493–501.
[59] G. Sonavane, K. Tomoda, A. Sano, H. Ohshima, H. Terada, K. Makino, Colloids Surf. B 65 (2008) 1–10.
[60] I. Fratoddi, I. Venditti, C. Battocchio, G. Polzonetti, F. Bondino, M. Malvestudto, E. Piscopiello, L. Tapfer, M.V. Russo, J. Phys. Chem. C 115 (2011) 15198–15204.
[61] M. Quintiliani, M. Bassetti, C. Pasquini, C. Battocchio, M. Rossi, F. Mura, R. Matassa, L. Fontana, M.V. Russo, I. Fratoddi, J. Mater. Chem. C 2 (2014) 2517–2527.
[62] L.A. Austin, M.A. Mackey, E.C. Dreaden, M.A. El-Sayed, Arch. Toxicol. 88 (2014) 1391–1417.
[63] S.C. Coelho, M. Rangel, M.C. Pereira, M.A.N. Coelho, G. Ivanova, Phys. Chem. Chem. Phys. 17 (2015) 18971–18979.
[64] S. Avvakumova, M. Colombo, P. Tortora, D. Prosperi, Trends Biotechnol. 32 (2014) 11–20.
[65] S. Krishnendu, S.A. Sarit, K. Chaekyu, L. Xiaoning, V.M. Rotello, Chem. Rev 112 (2012) 2739–2779.
[66] P. Chakkarapani, L. Subbiah, S. Palanisamy, A. Bibiana, F. Ahrentorp, C. Jonasson, C.J. Johansson, Magnetism Magn Mat. 380 (2015) 285–294.
[67] D.A. Giljohann, D.S. Seferos, W.L. Daniel, M.D. Massich, P.C. Patel, C.A. Mirkin, Angew. Chem. Int. Ed. 49 (2010) 3280–3294.
[68] M.S. Khan, M. Priyadarshini, S. Sumbul, B. Bano, Acta Biochim. Pol. 57 (2010) 499–503.
[69] H.I. Labouta, D.C. Liu, L.L. Lin, M.K. Butler, J.E. Grice, A.P. Raphael, T. Kraus, L.K. El-Khordagui, H.P. Soyer, M.S. Roberts, M. Schneider, T.W. Prow, Pharm. Res. 28 (2011) 2931–2944.